

# BIO-NANOCRYSTAL STABILIZED BIOSURFACTANT FOAMS FOR GROUNDWATER AND SOIL REMEDIATION

Alirza Orujov 📵, Behbood Abedi 📵, Karen Wawrousek 📵, Saman A. Aryana 📵

Chemical and Biomedical Engineering, University of Wyoming, Laramie, WY, USA

## Correspondence to: Saman A. Aryana, saryana@uwyo.edu

#### **How to Cite:**

Orujov, A., Abedi, B., Wawrousek, K., & Aryana, S. A. Bio-nanocrystal Stabilized Biosurfactant Foams for Groundwater and Soil Remediation. InterPore Journal, 2(1), IPJ260225–5. https://doi.org/10.69631/ ipj.v2i1nr36

RECEIVED: 18 July 2024 ACCEPTED: 20 Jan. 2025 PUBLISHED: 26 Feb. 2025

#### **ABSTRACT**

Surfactants are crucial for reducing surface tension at liquid interfaces and have diverse applications in various fields. Solutions of surfactants can help remediate contaminated soil and groundwater. Foams, dispersions of gas bubbles within a liquid stabilized by surfactants, exhibit enhanced sweep properties that can improve the cleaning efficiency in groundwater remediation. However, surfactant-stabilized foams are thermodynamically unstable, and this poses challenges to their applications. Utilizing nanoparticles in conjunction with surfactants has shown promise in enhancing foam properties and contaminant recovery. Biosurfactants, which are surfactants naturally produced by microorganisms, offer a promising alternative to synthetic surfactants due to their biodegradability and low toxicity. In this paper, we investigated the use of biosurfactants, specifically rhamnolipids, in combination with bio-nanocrystals, namely cellulose nanocrystals (CNCs), to improve foaming properties and assess contamination recovery through foam flooding tests. The effect of pH and CNCs on the foaming properties of the rhamnolipid solution was also examined. Foam stability and foamability were evaluated using modified bulk foam tests, considering foam stability parameters and maximum foam volume. Constant shear rate and strain amplitude sweep tests were performed on different foams formulated at varying pH levels to assess viscosity and elasticity, and to distinguish the foam exhibiting superior properties. Furthermore, sand pack flooding experiments were conducted to assess the performance of rhamnolipid-stabilized foams in groundwater remediation. The results reveal pH-dependent variations in the foaming properties of the mixture. The findings suggest that an optimal, eco-friendly foam with maximum stability, foamability, and elasticity can be formulated by using 1000 mg/L rhamnolipid together with 1000 mg/L CNCs at a pH value of 10. Additionally, experiments demonstrate that foams with optimal properties can recover approximately 70% of contaminants (n-decane), representing more than three times the recovery achievable through the same amount of water injection.

Orujov et al. Page 2 of 20

#### **KEYWORDS**

Bio-surfactants, Bio-nanoparticles, Nanoparticle-stabilized foams, Groundwater remediation, Soil remediation



This is an open access article published by InterPore under the terms of the Creative Commons Attribution-NonCommercial-NoDerivatives 4.0 International License (CC BY-NC-ND 4.0) (https://creativecommons.org/licenses/by-nc-nd/4.0/).

## 1. INTRODUCTION

Soil and groundwater may become contaminated to accidental discharge of contaminants such as petroleum products during their production, transportation, and storage, thereby impacting the long-term quality of groundwater and soil (11, 21, 67). Therefore, addressing soil and groundwater contamination is essential for preventing long-term impacts on the environment. In general, contaminant remediation techniques can be divided into chemical, physical, and biological methods (32). Among these remediation techniques, chemical methods like in situ chemical oxidation (ISCO) are widely regarded as the most effective means for addressing

#### **KEY POINTS:**

- Rhamnolipid- and cellulose nanocrystalbased foams were formulated for groundwater and soil remediation.
- Optimal pH and constituent concentrations were determined to achieve high stability and foamability.
- Foam flooding tests on sand pack samples demonstrated the foams' effectiveness for remediation.

petroleum and hydrocarbon product contamination (70). However, chemical methods may require additional treatment due to the chemical residues produced during the remediation process (32). Physical remediation methods, categorized as in situ or ex situ, often involve excavating contaminated sites or displacing non-aqueous phase liquids. These approaches can be costly and may have limited efficiency due to technological constraints (46, 64). In contrast, biological methods, while limited in applicability and influenced by numerous factors, offer an environmentally friendly treatment option that can be applied to large, contaminated areas, mitigating some of the concerns associated with traditional chemical and physical treatment methods (32). This work aims to combine the best aspects of physical and chemical approaches while minimizing their respective drawbacks.

Biological in situ degradation of hydrocarbon products relies on the introduction of specific microorganisms to contamination site (30). Certain microorganisms utilize hydrocarbon products as a carbon source and can biodegrade them into harmless substances, such as CO<sub>2</sub> and H<sub>2</sub>O (26). Despite their numerous advantages, biological methods are known to be time-consuming and their efficiency highly dependent on environmental conditions such as pH levels, temperature, salinity, type of contaminant, and other factors (32).

An alternative method that may overcome these disadvantages involves injecting a biodegradable surface-active agent (surfactant) to reduce the surface tension at the liquid-gas interface and increase the solubility of the contaminant (13, 48, 68). Surfactants, which can be petroleum-based or bio-based in origin (63), are amphipathic molecules that lower the surface tension between two liquids or a liquid and gas (48). Historically, in situ remediation has involved flooding the contamination sites with selected petroleum-based (synthetic) surface-active agents (surfactant flooding) (13). To date, petroleum-based surfactants have been primarily used due to availability and cost.

Research and development on biosurfactants has recently increased significantly. Biological or biosurfactants are produced by microorganisms such as yeast, bacteria, or fungi and are generally classified by their chemical compositions and molecular weights (63). Certain microbes naturally produce biosurfactants to access substrates for growth that are not miscible with water. Rhamnolipids are a class of biosurfactants composed of rhamnose sugar head groups and 3-(hydroxyalkanoyloxy) alkanoic acid (HAA) tail groups. Rhamnolipids are produced at high levels by the bacterium *Pseudomonas aeruginosa*,

Orujov et al. Page 3 of 20

with production of up to 240 g/L rhamnolipids in a fed-batch culture (9). The low interfacial tension of 0.25 mN/m (14) makes rhamnolipids interesting for use in foams, and they have been explored for use in oil recovery (12). While these properties alone make rhamnolipids interesting for remediation, the economical production of rhamnolipids has also been explored (9, 33, 56, 61), furthering their potential for use in remediation processes.

Groundwater remediation and enhanced oil recovery (EOR) share several similarities in their methods and challenges. Both processes involve injecting fluids to mobilize and extract target substances from near-surface or subsurface porous media. The primary distinctions lie in considerations of temperature, pressure, and resident fluid properties, as well as their objectives: groundwater remediation focuses on removing contaminants and pollutants, whereas EOR aims to enhance resource extraction from subsurface reservoirs (2). Surfactant flooding is a widely applied technique used in both groundwater remediation and EOR (17, 29, 36). Surfactant flooding techniques are based on lowering the interfacial tension between liquid interfaces, such as oil and water, and directing residual oil to production wells (17). Among various surfactant flooding methods, Foam-Assisted Surfactant Flooding (FASF) is a method known for its several advantages (36); FASF combines the reduction of liquid-liquid interfacial tension to significantly low levels where foaming of the gas can control gas mobility (36, 49). However, surfactantstabilized foams show some instabilities due to the gravitational drainage and diffusion-induced foam coarsening at subsurface applications, particularly in presence of oil (18, 41, 52). These challenges may be mitigated by adding nanoparticles such as silica, fly ash, and iron oxide. (28). The stability of foams is significantly influenced by the characteristics of nanoparticles (NPs) incorporated into the system. Key factors include nanoparticle size, concentration, and the pH of the solution (4, 52). Although each of these multiple factors usually has a combined effect on foam stability, smaller nanoparticles usually have a positive effect on foam stability when other factors are kept constant. Smaller nanoparticles have a higher surface area-to-volume ratio, which enhances their ability to adsorb at the gas-liquid interface, thereby stabilizing the foam (16, 39, 76).

Increasing the concentration of nanoparticles generally enhances foam stability up to a certain point in a given concentration of particular surfactant. Higher concentrations provide more particles to adsorb at the gas-liquid interface, forming a robust barrier against bubble coalescence (59, 72) with and without the presence of oil (52). However, beyond an optimal concentration, excess nanoparticles can lead to aggregation or increased viscosity, which may adversely affect foam stability (35).

The pH of the solution affects the surface charge and dispersion stability of nanoparticles. At certain pH levels, nanoparticles may aggregate due to reduced electrostatic repulsion, leading to decreased foam stability. Adjusting the pH can modify the surface properties of nanoparticles, influencing their interaction with surfactants and the gas-liquid interface (45). Researchers have focused on formulating an optimal foam by conjugating different surfactant molecules and nanoparticles. Wang et al. (67) used fly ash and alpha-olefin sulfonate (AOS), and lauramidopropyl betaine (LAPB) mixture to formulate a foam for soil remediation and found an optimal concentration of nanoparticles for highly stable foam. Similarly, Guo and Aryana (27) formulated highly stable CO<sub>2</sub> foams using silica and nano clay with LAPB and AOS mixtures. Microfluidic experiments showed that more than 90% of the oil may be recovered by foams formulated with LAPB-AOS mixtures (27).

Although subsurface application of nanoparticles has several benefits, their toxicity and environmental impact have been a cause for concern (53, 54). Metal oxide nanoparticles such as  $TiO_2$ ,  $ZnO_2$ , and  $Fe_3O_4$  are among the most used engineered nanoparticles in different fields. Most of these nanoparticles have been reported to show inverse health effects on humans and other living organisms. Grassian et al. (25) reported a significant inflammatory response when mice were exposed to 7.22 mg/m³  $TiO_2$  nanoparticles for 4 hours each day over a total duration of 10 days. The study also showed that these nanoparticles can be suspended in air and form aerosol particles, which can be inhaled and cause an immune response (25). In their study, Karlsson et al. (37) reported cell viability and DNA damage, as well as cytotoxicity associated with exposure to ZnO and  $TiO_2$  nanoparticles at a concentration of 40  $\mu$ g/cm².

Orujov et al. Page 4 of 20

Alternatively, nanomaterials such as cellulose nanocrystals (CNCs) are primarily obtained from low-cost, renewable resources and are used for various healthcare applications (58). Cellulose is a fibrous, tough, water insoluble polymer of glucose molecules. Cellulose is the most abundant polymer naturally present in plants, algae, fungi, and some bacteria (22). Cellulose nanocrystals are produced from bulk cellulose, usually involving acid hydrolysis to break down the cellulose structure (10) to form nanocrystals (15). Cellulose nanocrystals consist of cellulose chain segments with an almost perfect crystalline structure and exhibit high specific strength, surface area, and other unique properties (22). Therefore, CNCs can be an alternative for toxic and economically costly metal oxide nanoparticles, especially for remediation.

In this work, we used rhamnolipid biosurfactant, together with CNCs, to formulate highly stable foams that can be used for soil and groundwater remediation. While employing foam flooding can mitigate adverse effects like gravitational segregation and viscous fingering, integrating biological surfactants with nanoparticles aims to minimize environmental impacts during groundwater and soil remediation. In this lab scale study, we investigated the effects of pH, surfactant, and CNC concentration on foam stabilities for obtaining optimal foams. Their effectiveness in remediation was also investigated through foam flooding experiments.

## 2. MATERIALS AND METHODS

# 2.1. Rhamnolipid CMC measurements, the effect of PH

A commercially available 90% pure rhamnolipid surfactant a was used as the foaming agent. In porous media settings, foam stability depends on surfactant concentration, critical micelle concentration (CMC), electrolyte concentration, and the ability of surfactant to form black films (5). Among these, CMC is a key parameter in governing the stability and foamability of surfactant-stabilized foams (44). Critical micelle concentration is defined as the maximum solubility of a monomer at a particular solution, and at CMC, surfactant molecules start to aggregate and form micelles. To achieve optimal performance, the surfactant concentration must significantly exceed the CMC, often by several orders of magnitude. This is because surfactant molecules preferentially absorb fluid-fluid interfaces. The presence of micelles in the bulk solution, even when these interfaces are present, indicates that the interfaces are saturated with surfactant molecules. Such saturation ensures that the surface tension at the interfaces has reached its minimum possible value (19, 59, 75). The presence of impurities, ions, and the pH of the solution influence the CMC, which in turn affects foamability (19, 44). Therefore, understanding the ionic strength of the solution and accurately measuring the CMC values are fundamental steps in formulating stable foams. During our experiments, deionized (DI) water was used for simplicity. However, the pH of the solution was modified using 4, 7, and 10 color-coded pH buffer solutions<sup>b</sup>. Reported CMC values for mono and di-rhamnolipids and their mixtures usually range from 1 to 500 mg/L (7, 57, 69). The CMC values can be determined by measuring the equilibrium surface tension of surfactant-containing solutions at various surfactant concentrations. At the CMC, the solution achieves a minimal surface tension (y), and further addition of surfactants no longer affects the surface tension (69). To determine the CMC value for a rhamnolipid solution at three different pH levels, the surface tension of a series of surfactant concentrations was measured using a force tensiometer<sup>c</sup> and the plate method.

Critical micelle concentration measurements can also be conducted using the dynamic light scattering (DLS) technique. Topel et al. (62) compared CMC measurements obtained from fluorescence spectrometry and DLS for polybutadiene-block-polymer systems. Their results demonstrate that CMC values obtained from DLS are as sensitive as those obtained from fluorescence spectrometry (62). According to their study, the intensity of scattered light remains constant at concentrations below the CMC, whereas it increases linearly above it. This phenomenon occurs because the concentration of surfactant affects the amount of scattered light, leading to a proportional increase in the count rate. While DLS is an easy-to-handle technique that can be utilized for CMC measurements of surfactants and

<sup>&</sup>lt;sup>a</sup> AGAE technologies ®, R90

<sup>&</sup>lt;sup>b</sup> Fischer Chemical

<sup>&</sup>lt;sup>c</sup> KRÜSS scientific, K100

Orujov et al. Page 5 of 20

polymers, it is essential to consider its limitations (23). Hence, in addition to surface tension experiments, DLS measurements, including average hydrodynamic diameter and scattered light intensity, were performed over a range of rhamnolipid concentrations at neutral pH to compare and corroborate the results. In this work, a Brookhaven Zeta PALS instrument was employed to obtain the average hydrodynamic diameter and light intensity. The results obtained from these measurements are reported and further discussed in the results and discussion section. The secondary objective of conducting DLS measurements to determine the CMC is to evaluate the efficacy of this method in relation to established techniques like the surface tension method. Due to inconsistent DLS measurements, surface tension measurements were exclusively used to determine CMC values.

#### 2.2. CNCs and effect of sonication

Although the stability of foams depend on the combination of multiple factors, including nanoparticle size, investigations into the size-dependent properties of SiO<sub>2</sub> and AlOOH nanoparticles have revealed that nanoparticles with smaller sizes tend to generate overall more stable foams compared to those with larger sizes (16, 39, 74). Conversely, CNCs are characterized by their high aspect ratios and polydisperse size distribution, making them prone to rapid aggregation in solution. An effective strategy to mitigate this adverse effect is to break down CNCs into more uniform pieces by introducing energy. Sonication has been identified as the most effective method for achieving this, thereby increasing the stability of CNCs in solution (38). Previous studies have also demonstrated that nanoparticle concentration plays a significant role in foam stability. Optimal nanoparticle concentrations for foam stabilization have been observed for silica, iron oxide, and fly ash nanoparticles, typically around 1000 ppm (28, 31). Therefore, in this study, CNCs were subjected to sonication at different concentrations, and the impact of sonication on the average particle size was investigated. This approach aimed to assess how sonication influenced the dispersion and stability of CNCs in solution, potentially providing insights into optimizing CNC-based foam formulations. This study employed commercially available CNCs sourced from Nanografi® with an average particle size of 10-20 nm in width and 300-900 nm in length. The powder form of CNCs was dispersed in DI water under continuous stirring at 500 rpm using a magnetic stirrer for a duration of 24 hours. Following the stirring period, the samples were allowed to settle for additional hours before being subjected to sonication using a probe sonicator<sup>d</sup> at varying amplitudes and energies. To maintain the integrity of the solution and prevent evaporation or compositional changes, a dry ice bath was applied around the sonicated sample. Subsequently, the average hydrodynamic diameters of the samples were measured using a Brookhaven Zeta PALS instrument, which employs the DLS technique at room temperature. The obtained results are presented in the results section, providing insights into defining an optimal sonication time for future experiments.

# 2.3. Foam properties

Foam stabilities and foamability are commonly assessed using bulk foam tests, where foam stability refers to the duration it takes for the foam to decrease to half of its initial volume or height in a cylinder, while foam foamability represents the maximum amount of foam generated initially. Both parameters can be evaluated simultaneously in modified bulk foam tests (28). However, these measurements, particularly foam half-life, often require extended durations, posing experimental challenges (31). To address this, additional parameters known as R5 and R60 can be employed to assess foam stability within a shorter timeframe. The parameters R5 and R60 are defined as follows (43):

```
\begin{split} R_5 &= \frac{\textit{Foam height (t=5 min)}}{\textit{Initial foam height '}}, \\ R_{60} &= \frac{\textit{Foam height (t=60 min)}}{\textit{Initial foam height}}. \end{split}
```

Higher values of R5 and R60 indicate enhanced stability, while the maximum foam volume shows foamability. In this study, R5, R60, and maximum foam volume were evaluated for foams at three different pH levels, three rhamnolipid concentrations (500, 1000, and 1500 mg/L), and four CNC concentrations (0, 500, 1000, and 15000 mg/L). The tests were conducted using 20 mL solutions in a 100

<sup>&</sup>lt;sup>d</sup> QSonica, Q700

Orujov et al. Page 6 of 20

mL graduated cylinder, with a camera recording the initial foam volume and its degradation over a one-hour period. Bulk foam properties were evaluated using the modified bulk foam testing method described by Guo et al. (28). This method involves vigorously shaking a graduated cylinder for a specified duration or until the maximum foam volume is achieved, after which the foam decay rate was carefully analyzed. In all experiments, air was used for foam generation. The choice of this foam generation technique was primarily driven by the need to maintain consistency between the rheology and foam stability experiments. The results obtained are discussed in detail in the results and discussion section.

# 2.4. Viscoelasticity of foam

Viscoelasticity has a direct impact on the sweep efficiency of injected fluids in porous media. Viscoelastic fluids can elongate and deform as they flow through porous media, enabling them to reach low permeability regions. We conducted an amplitude sweep test using a strain-controlled rheometere to measure foam viscoelasticity. A cup and vane geometry was implemented. Due to the nature of foams, and based on our experience, we selected this relatively short and informative test. Foams were prepared with 1000 mg/L Rhamnolipid and 1000 mg/L CNCs at pH values of 4, 7, and 10 inside the cup before performing the tests. A 10 ml initial sample was taken for each experiment, and the cup was shaken rigorously for 1 minute to form a foam. In an oscillatory test, the vane is fixed while the cup oscillates back and forth. The amplitude of oscillation (how far the moving cup moves back and forth) gradually increased from 1 to 100%, while keeping the frequency (rate of oscillation) constant at 10 rad/s. This means the material experiences increasing strain. Then, we monitored the evolution of storage modulus (G') and loss modulus (G"). These moduli are crucial for understanding the viscoelastic behavior of materials under strain. Their interpretation provides insights into the material's structure and performance. A high G' value suggests that the material is more elastic, meaning it can withstand higher elastic deformations viscoelastically. A high G" value indicates that the material is more liquid-like or viscous, thus it flows and deforms readily under stress, with a significant amount of energy being lost **(1)**.

Similarly, the viscosity of the foam at a constant shear rate of 10 s<sup>-1</sup> was measured as a function of time. The same test procedure was applied: a 10 mL initial sample was placed in a cup and shaken rigorously for 1 minute to form foam. This test serves as a simple, quick-check method to compare the viscosity differences of various foams and observe their decay over time. Foams can enhance contaminant recovery by increasing the viscosity of the displacing fluid, thereby reducing the mobility ratio between the resident non-aqueous phase liquid (NAPL) and the displacing foam and improving displacement efficiency (42).

# 2.5. Sand pack preparation and saturation

The cleaning efficiency of foam flooding is often evaluated using contaminated soil or core samples to simulate the targeted formation. Sand packs are commonly utilized for soil and groundwater remediation experiments due to their cost-effectiveness and the reproducibility of core sample properties. In this study, artificial sand packs were prepared by modifying an existing sand pack consolidation method from the literature (65). The sand packs comprised Northern-White monocrystalline sand with a grain size distribution corresponding to 100 mesh size, ranging from approximately 0.15 mm to 0.4 mm in diameter. This sand is known for its high purity (100 %SiO2), sphericity (0.8), and crush resistance, and is used for hydraulic fracturing in the oil and gas industry. Figure 1 shows the sand packing and saturation procedure.

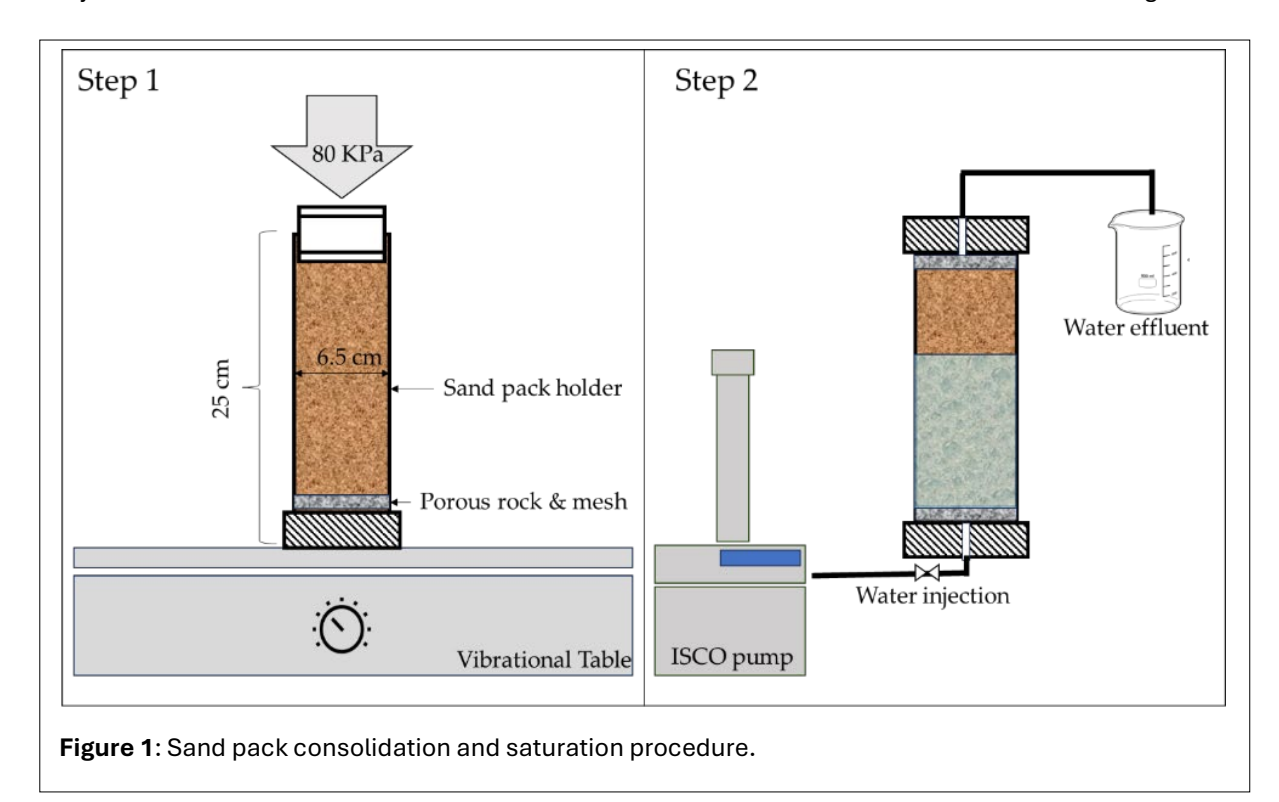
The dry sand consolidation process involved using a vibrational table at the medium vibrational frequency for over an hour. The sand column was secured with porous rocks and 100-mesh metal meshes at each end. The pack was saturated by injecting water from the bottom up by holding the sample vertically. An ISCO pump<sup>g</sup> was used for water injection at a rate of 1 mL/min, and at least three pore

<sup>&</sup>lt;sup>e</sup> TA Instruments<sup>©</sup>, ARES G2

f Carbo®

g Teledyne ISCO 1000D

Orujov et al. Page 7 of 20



volumes (PV) water were injected. Porosity and permeability values were calculated based on the methods described in literature (51).

In this study, consolidating the sand packs was essential to create struc-tureally integrated samples with controlled permeabil-ity and consistency across experiments. This approach ensured uniform porosity and permeability across all sand packs, enabling us to isolate and evaluate the specific effects of foam treatments without introducing additional variability from differences in the porous media properties. Moreover, it's important to note that laboratory-consolidated sand packs typically exhibit higher permeability than naturally occurring consolidated rocks such as sandstone.

# 2.6. Foam flooding experiments

For groundwater remediation experiments, a "pre-generation" foam injection method was employed (71). This injection method involves generating foam using a foam generator before the injection process. The pre-generation method is particularly advantageous for high permeability porous media, such as sand packs, because it can create a higher pressure drop at the inlet (6). **Figure 2** illustrates the experimental setup for pre-generation foam injection.

The experimental setup comprises a syringe pump<sup>h</sup> utilized for injecting both the contaminant and surfactant solution. Pre-generated foam was injected into sand-packed columns measuring 6.5 cm in diameter and 25 cm in height, as shown in **Figure 2**. In laboratory studies, researchers frequently use single, well-characterized compounds as model contaminants in the form of NAPLs (47). This approach allows for the isolation of specific variables and mechanisms without the complexities introduced by mixtures of contaminants. For example, normal-decane (n-decane), a straight-chain alkane, is commonly selected due to its representative properties among aliphatic hydrocarbons (3, 8, 40). This simplification facilitates a more controlled investigation of contaminant behavior and remediation strategies. Normal-decane, a straight-chain alkane, served as the representative non-aqueous phase liquid (NAPL) contaminant during the experiments. Following full saturation of the sand pack with water, decane was horizontally injected at a rate of 1 mL/min using the syringe pump until it was produced at the outlet. The injection scheme was designed to mimic a real-life scenario where the contaminant gradually migrates from the contamination source to the aquifer. The quantity of contaminant within the sand

-

h PHD ULTRA TM

Orujov et al. Page 8 of 20

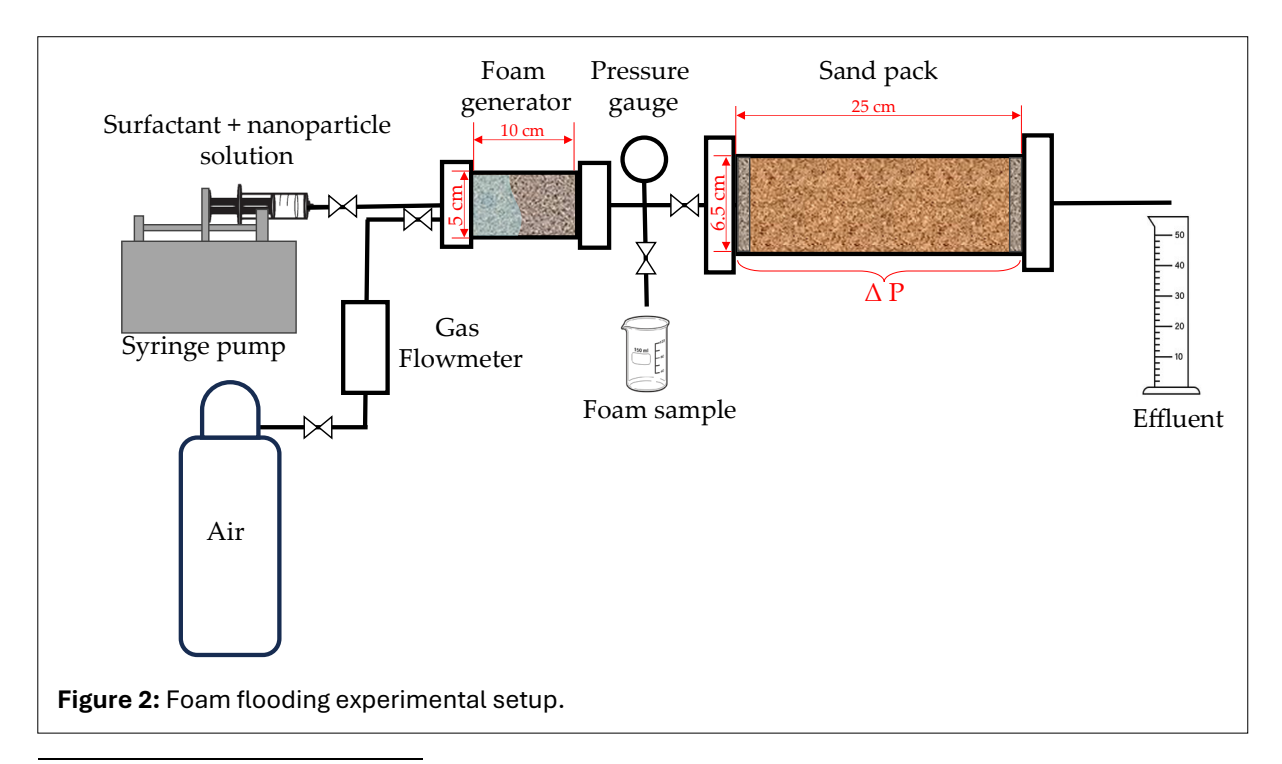
pack is then recorded by subtracting the produced NAPL from initial quantity prior to commencing the foam flooding process.

Aranda et al. (6) investigated foam injection across various porous media with different permeability ranges. According to their study, the permeability of foam generators does not significantly impact the final results. In fact, foam generators with higher permeability may offer advantages by reducing excessive injection pressures in both field and laboratory settings. Therefore, in this study, foam generation employed coarse-grained sand with a wide grain size distribution. Foam was generated by co-injecting air at a flow rate of 100 mL/min along with the surfactant and CNC mixture solution at a flow rate of 1 mL/min. The distinct separation between the two liquids was visually observed in a graduated cylinder at the sand pack outlet, where their immiscibility created a clear interface, with n-decane forming the upper layer and water the lower layer. The process was monitored using a digital camera<sup>i</sup> to record the recovery of contaminant and the pressure drop by using a digital pressure gauge<sup>j</sup> with ± 0.05 accuracy at the inlet of the sand pack. Subsequently, the relevant data was obtained for analysis.

# 3. RESULTS AND DISCUSSION

# 3.1. Rhamnolipid CMC measurements, the effect of pH

Surface tension measurements at a wide range of concentration and pH values was performed to determine the critical micelle concentration (CMC) of the surfactant solutions. **Figure 3a**, shows the results from surface tension measurements over a series of rhamnolipid concentrations at pH values of 4, 7 and 10. At the CMC, the solution obtains the minimum surface tension, and adding more surfactants does not affect the surface tension of the solution. Experimental findings presented in **Figure 3a** indicate that the CMC of rhamnolipid increases with rising pH levels. Specifically, the CMC values were approximately 50 mg/L at pH 4, 200 mg/L at pH 7, and 500 mg/L at pH 10. This is likely due to the presence of the carboxyl group in rhamnolipid, which gives it an anionic character dependent on pH. At lower pH values, the carboxyl groups are protonated, making the surfactant molecules more hydrophobic and promoting micelle formation at lower surfactant concentrations. At higher pH, however, most of the carboxylic groups are deprotonated, resulting in more negatively charged



<sup>&</sup>lt;sup>i</sup> Logitech c270

i

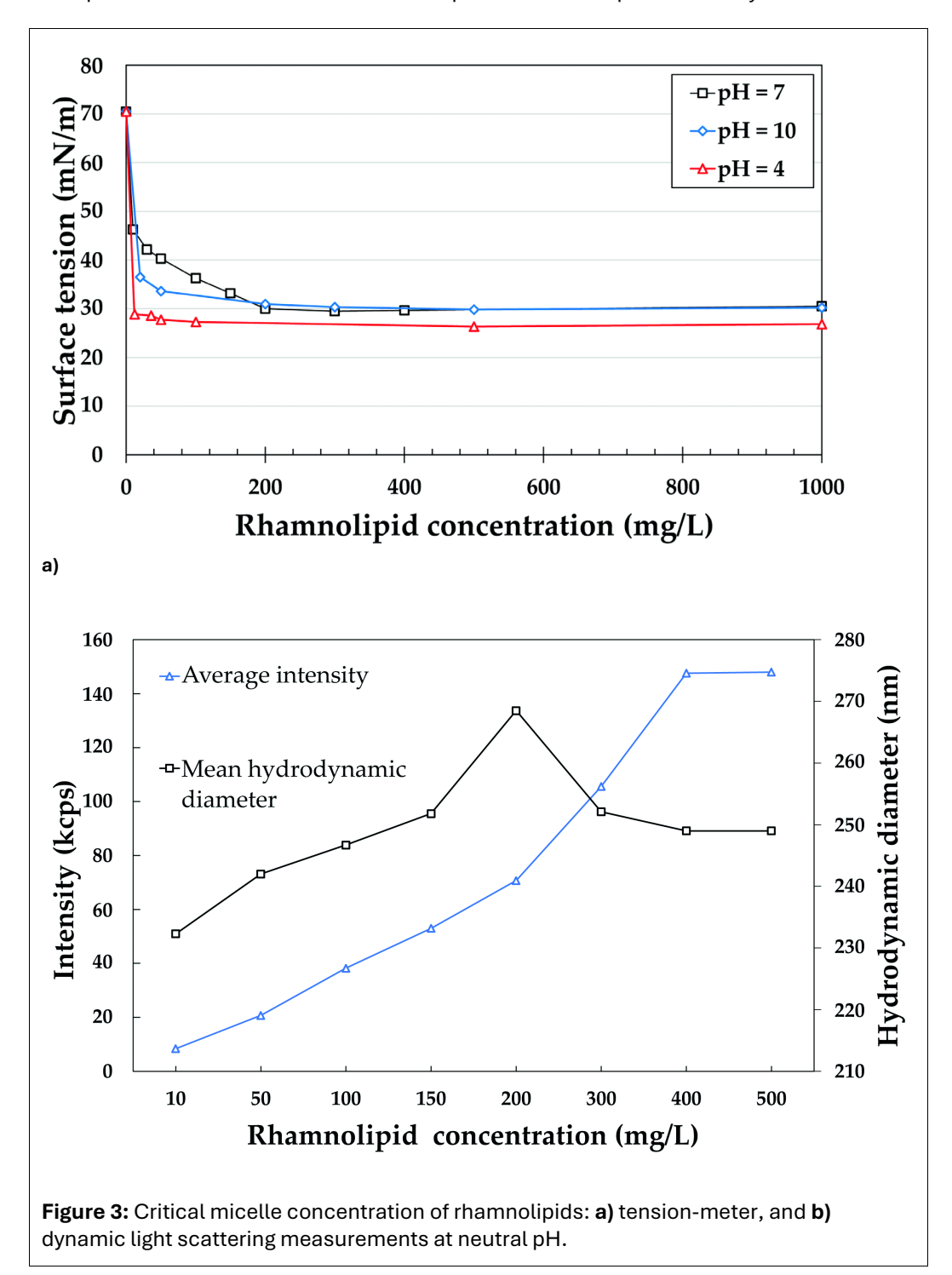
j ASHCROFT

Orujov et al. Page 9 of 20

surfactant molecules. This increased negative charge results in higher repulsion among molecules and leads to higher CMC values (34, 50). Despite the change in CMC due to pH difference, surface tension values above CMC ( $\sigma_{cmc}$ ) were not considerably different and were observed to remain around 29 mN/m. Since optimal foaming properties can be obtained above CMC concentrations, 500, 1000, and 1500 mg/L rhamnolipid concentrations were chosen for the foaming experiments.

The CMC for rhamnolipid at a neutral pH was also investigated using DLS measurements. **Figure 3b**, shows that there is a noticeable change in the intensity of scattered light and the hydrodynamic diameter at approximately 200 mg/L, which corresponds to the measured CMC value using a tensiometer.

Although there was an observable change in the intensity of scattered light and the hydrodynamic diameter of particles at the CMC of the rhamnolipids, this technique does not yield accurate results for

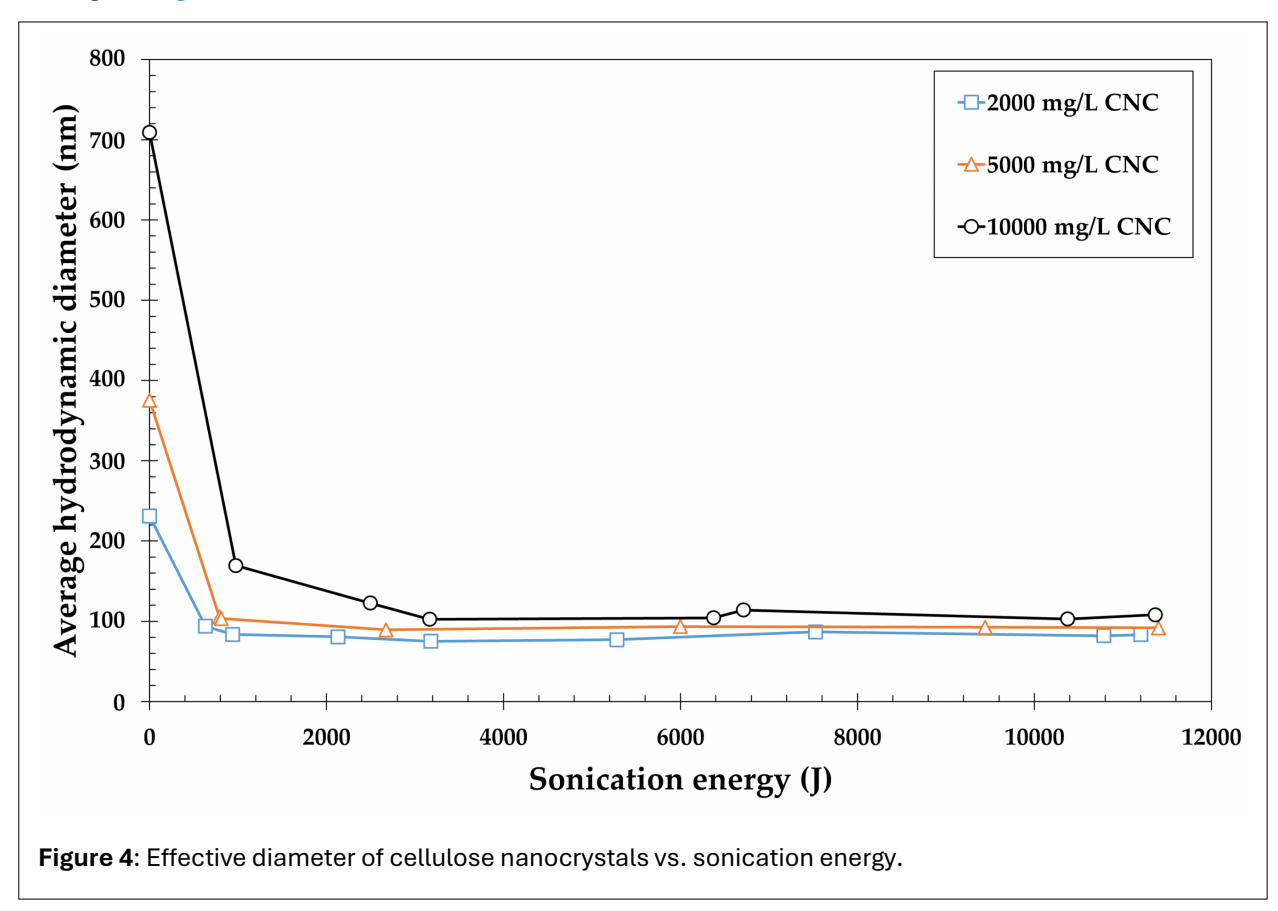


Orujov et al. Page 10 of 20

determining low CMC values. The sensitivity of DLS instruments for CMC measurements depends on several factors, such as the light transmissivity of the sample, the ability to mitigate multi-scattering phenomena at high sample concentrations, and the intrinsic resolution limitations of DLS, which can restrict its capability to distinguish particles differing in size by less than a factor of 3 (39).

## 3.2. CNCs and effect of sonication

As previously described, the mixtures are sonicated to promote optimal dispersion of CNCs in the solution and more stable foams. Here, we investigate the minimum input sonication energy to achieve this goal. **Figure 4** illustrates the results from the sonication of 10 mL CNCs in solution.



From **Figure 5**, it is evident that cellulose nanorods can be broken down into an average hydrodynamic diameter of approximately 100 nm through proper sonication. This step is particularly important as the particle size can significantly influence foam stabilization processes. Therefore, for the subsequent experiments, all CNC particle solutions underwent sonication with sufficient energy to achieve particle sizes of approximately 100 nanometers.

The technoeconomic considerations for foam injection in near-surface remediation and subsurface resource recovery scenarios are likely different. This work investigates the technical feasibility of contaminant removal and remediation using bio-based foam systems. However, it is important to note that economic considerations, which fall outside the scope of this study, will ultimately guide their practical application. According to the results of experiments reported in **Figure 4**, approximately 1 kJ of energy is required to break down a 10 mL solution containing 100 mg of CNC nanocrystals (10,000 ppm). While this energy consumption may be minimal, the economic feasibility of the process depends on several factors, including geographic considerations, energy costs, and materials preparation techniques (e.g., dry versus wet milling).

Orujov et al. Page 11 of 20

# 3.3. Foam properties

The foam properties, specifically foamability and foam stability, were evaluated in relation to pH, rhamnolipid concentration, and CNC concentration. The results below demonstrate that foam properties exhibit a notable dependency on pH, as well as the concentrations of rhamnolipids and CNCs. As previously stated, R5 and R60 quantify foam stability, measured by decay time, while maximum foam volume indicates foamability. Hence, aiming for higher values of these parameters is desirable when formulating foams to achieve superior overall properties. **Figure 5** shows R5, R60 and maximum foam volume (mL) for foams with different rhamnolipid and CNC concentration at pH values of 10, 7 and 4.

From **Figure 5a**, maximum R5, R60, and maximum foam volumes were observed for foams formulated using 1000 mg/L of CNCs and 1000 mg/L of rhamnolipids. Remarkably, the foam formulated by 1000 mg/L rhamnolipid together with 1000 mg/L CNCs at a pH value of 10 exhibited superior stability compared to all other formulations across various pH levels. Due to its stability, this specific foam formulation was selected for foam flooding experiments. Similarly, **Figure 5b** illustrates the foam stability parameters R5, R60, and the maximum foam volume at a neutral pH. Foams at a neutral pH exhibit an

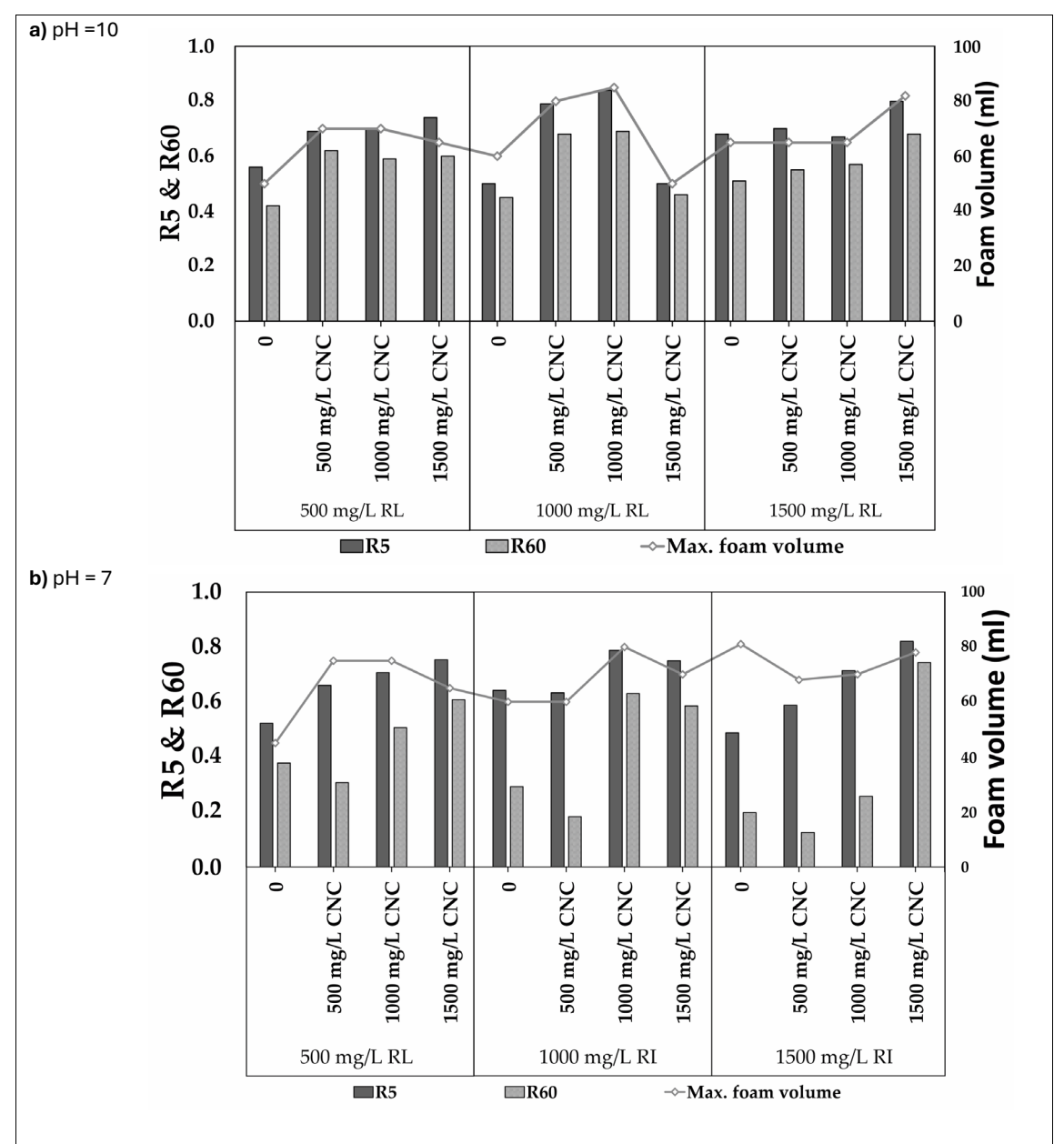


**Figure 5 (a,b):** Foam stability and foamability for various combinations of Rhamnolipid and cellulose nanocrystals (CNC) at a pH value of **a)10** and **b)** 7.

Orujov et al. Page 12 of 20

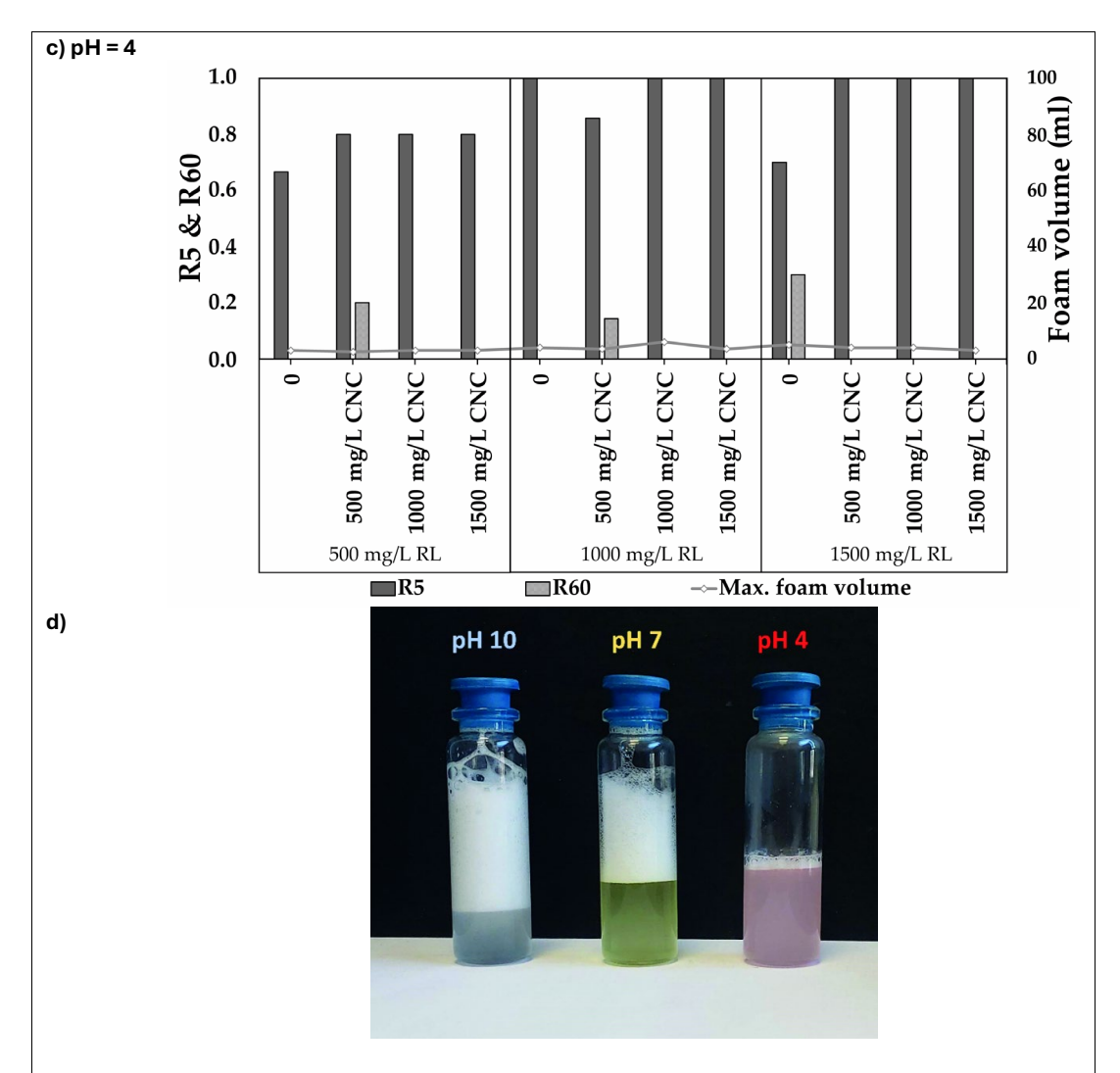


Figure 5 (c, d): Foam stability and foamability for various combinations of Rhamnolipid and cellulose nanocrystals (CNC) at a pH value of c) 4. d) Visual demonstration of foam volumes formulated with the 1000 mg/L of rhamnolipid and CNC, generated by simultaneously vigorous shaking for 1 minute.

overall inferior stability and foamability compared to those at a pH of 10. Foams generated at a pH value of 4 exhibited the least favorable stability and foamability when compared to foams generated at a neutral pH and a pH of 10. **Figure 5c** shows that the maximum foam volumes at a pH of 4 did not exceed 6 mL, and most of the foams decayed within an hour. This indicates that the environment with a pH of 4 adversely affected foam stability and foamability compared to neutral and alkaline conditions. **Figure 5d** visually demonstrates the foams formulated with 1000 mg/L rhamnolipid and 1000 mg/L CNCs at pH values of 4, 7, and 10. Each solution in **Figure 5d** has a volume of 10 mL, and all foams were generated by vigorously shaking the vials simultaneously for 1 minute, followed by a 30-second resting period.

The pH-dependent stability and foamability of rhamnolipid foams have been investigated in various studies, yielding similar results (24, 34, 50). The reduced foamability and stability of rhamnolipid foams at a low pH can be attributed to the reduced electrostatic repulsion between surfactant molecules (50). This reduction in repulsion leads to a decrease in the electrostatic charge on the surfactant films, resulting in a reduced ability to maintain bubble separation, ultimately causing the bubbles to collapse. Interestingly, excessive foaming is generally unfavorable for rhamnolipid fermentation processes, and therefore, foam control is often achieved by adjusting the pH (24). By optimizing the pH conditions, it is possible to regulate the foam formation and stability during rhamnolipid production, ensuring efficient fermentation processes.

Orujov et al. Page 13 of 20

# 3.4. Viscoelasticity of foam

Rheological properties of foams are directly relevant to their behavior in porous materials, and here we examine the foam's storage modulus (G') and loss modulus (G"). **Figure 6a** shows that the highest G' and G" values correspond to the foam formed at the highest pH, whereas the lowest pH produced negligible foam. This is consistent with the results, where G' is almost zero at pH 4.

On the other hand, the results in **Figure 6b** indicate that the foam formulated with 1000 mg/L CNC and 1000 mg/L rhamnolipid at a pH of 10 exhibits a higher viscosity compared to that at pH 7, which, in turn, is higher than at pH 4. Furthermore, the decrease in viscosity over time suggests that the foam at a pH of 10 exhibits higher foamability, with the reduction in viscosity attributed to foam bursting. In contrast, the foams at pH 7 and 4 demonstrate lower foamability compared to the foam at pH 10.

Considering the importance of elasticity, viscosity and elongational flow in porous media, it can be concluded that foams formed using 1000 mg/L rhamnolipid and 1000 mg/L CNCs at pH 10 will result in the highest sweep efficiency.

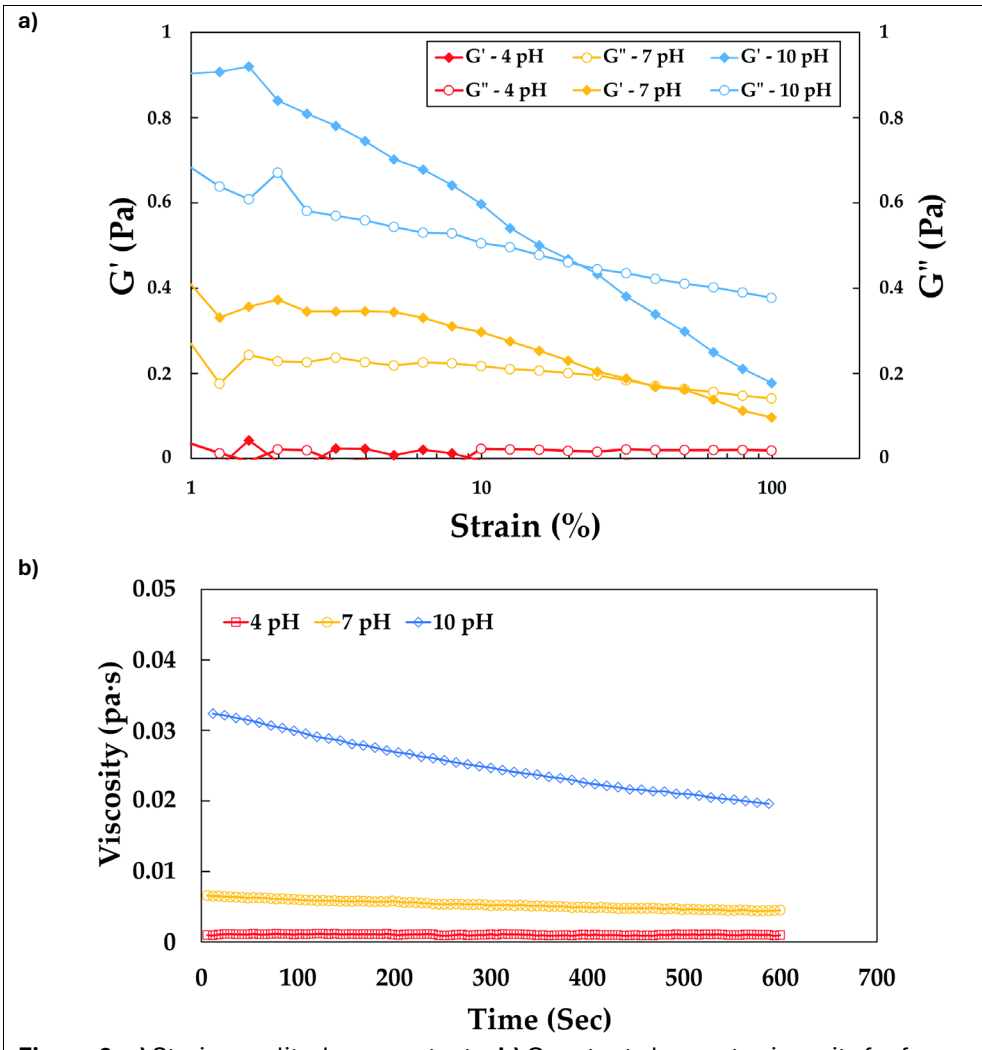


**Figure 6**: **a)** Strain amplitude sweep tests, **b)** Constant shear rate viscosity for foams with 1000 mg/L rhamnolipid and 1000 mg/L cellulose nanocrystals at pH values of 4, 7, and 10.

Orujov et al. Page 14 of 20

# Sand pack preparation and saturation

To simulate the impact of the rhamnolipid-CNC foams on hydrocarbon contaminated soils, sand packs were prepared and decane was introduced as the contaminant. Two identical sand packs were prepared and saturated for water and foam flooding using the consolidation technique described in Figure 1. **Table 1** shows the properties of the consolidated sand packs.

Table 1: Properties of sand packs used for flooding experiments.		
Properties	Sample 1	Sample 2
Core diameter (mm)	58.5	58.5
Length (mm)	228.6 (9")	228.6 (9")
Pore volume (L)	0.197	0.191
Porosity, Φ (%)	32±2	32±1
Steady state ΔP (psi)	0.5	0.8
Flow rate, Q (mL/min)	1	2
Water viscosity, $\mu$ (cP)	0.89	0.89
Permeability, K (mD)	416	833

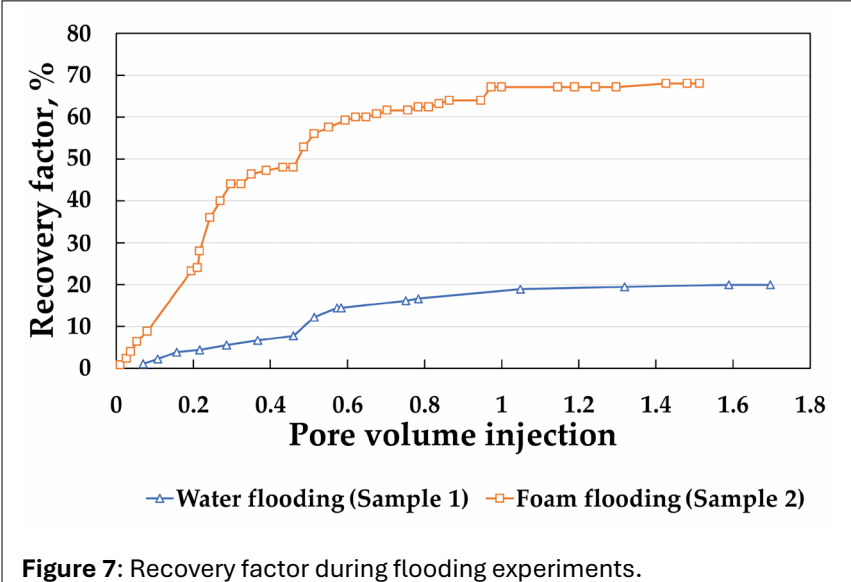
#### Foam flooding experiments 3.6.

After saturating the sand packs with a minimum of three pore volumes of water, decane was injected using a syringe pump at a flow rate of 1 mL/min. Approximately 100 mL of decane was injected for each sand pack sample before it was produced over the outlet. The sand pack samples (Sample 1 and Sample 2, as shown in Table 1) used for water and foam flooding were distinct and independent. Sand Pack Sample 1 was used for water flooding, while Sample 2 was used for foam flooding without prior water flooding. Subsequently, the recovery factor for water and foam injection was calculated at various pore volume (PV) injections, and the results are depicted in **Figure 7**.

The recovery factor was calculated as the percentage ratio of the displaced n-decane to the original amount of n-decane present in the system. Results show that 1 PV water injection can only recover around 20% of the decane. In contrast, 1 PV solution of rhamnolipid and CNCs mixture and air can recover around 70% of the contaminant.

The initial decane saturation in samples 1 and 2 was approximately 49% before both water and foam flooding. Multiple studies have conducted similar flooding experiments using rhamnolipid foams for soil and groundwater remediation. For instance, Wang and Mulligan (66) performed column experiments to assess the feasibility of using rhamnolipid foam for the removal of cadmium (Cd) and nickel (Ni) from contaminated sandy soil. Their findings demonstrated that a 0.5% rhamnolipid foam solution at pH 10.0

successfully removed 73.2% of Cd and 68.1% of Ni after flushing with 20 volumes of the solution. Similarly, Xue et al. (73) investigated the combined effect of rhamnolipids and bacterial consortia on the bioremediation of petroleum-contaminated Their results indicated that the addition of rhamnolipids significantly enhanced the rate and extent of petroleum hydrototal carbon biodegradation, achieving up to 81% removal within 35 days (73).



Orujov et al. Page 15 of 20

A more recent study by Zhu et al. (77), which conducted foam flooding experiments using glass beads and actual soil samples contaminated with a mixture of naphthalene and phenanthrene (both polycyclic aromatic hydrocarbons, PAHs), is particularly relevant to the use of rhamnolipid-based foam flooding for groundwater remediation and closely aligns with our study. Under optimal conditions, Zhu et al. achieved removal efficiencies of 60.1% for naphthalene and 56.68% for phenanthrene from soil samples. In laboratory-simulated media using glass beads, the removal efficiencies were even higher, with 76.69% for naphthalene and 70.43% for phenanthrene. The study utilized a surfactant mixture of rhamnolipid and fulvic acid in a 3:1 volume ratio and concluded that this combination significantly outperformed the use of either rhamnolipid or fulvic acid alone. Foams formulated solely with rhamnolipid achieved less than 55% recovery of PAH contaminants under optimal conditions, highlighting the limitations of using rhamnolipid-only foams for effective remediation (77). Considering this, our foam formulated with CNCs and rhamnolipid has demonstrated enhanced recovery properties, proving to be more effective.

A potential question that may arise concerns understanding the pH ranges of soil and groundwater encountered in real-life field scenarios, as these may affect the application of rhamnolipid foam performance. Globally, soil pH typically ranges from 3.5 to 9, with pH values above 9 indicative of strongly alkaline soils, which are rare (60). According to the US EPA, the permissible range for groundwater pH is approximately 6.5–8.5. However, contaminated groundwater may exhibit pH values outside this range (20). Although rare, studies have shown that corrosion of metal equipment, particularly in industrial sites, can lead to localized increases in groundwater pH above 10 (55).

Given the rarity of encountering a pH of 10 in natural conditions, this study focused on identifying the most favorable foam formulation by investigating foam properties under controlled conditions rather than replicating natural conditions. Additionally, the performance of the foam in field applications may depend on the generation method (e.g., in situ or ex situ), the resident fluids, and physical conditions. For instance, in a relevant study, Wang and Mulligan (66) found that rhamnolipid-based foam with optimal contaminant recovery properties could be formulated at an initial pH of 10, and the injection of this pre-generated foam into a soil column achieved the highest contaminant recovery (66). Future studies may explore the effects of additional factors on foam performance in field-scale applications.

#### 4. CONCLUSION

In conclusion, this study investigated the utilization of a biosurfactant, specifically rhamnolipids, in combination with bionanocrystals, namely CNCs, for the creation of stable foams applicable in groundwater and soil remediation. The study examined how various factors such as pH, CNC, and rhamnolipid concentrations influenced foam properties, and identified the optimal foam formulation exhibiting the highest foam volume and stability parameters, denoted as R5 and R60. It was observed that increasing the pH had a positive impact on foam properties. Consequently, foams formulated at a pH value of 10 demonstrated properties superior to those at a pH of 7 and 4.

The study identified an optimal foam that was formulated with 1000 mg/L rhamnolipids and 1000 mg/L of CNCs at a pH value of 10, exhibited an R5 value of 0.85, an R60 value of 0.69, and achieved a maximum foam volume of 85 mL under the specified test conditions. Furthermore, strain amplitude sweep tests confirmed that the foam exhibited high stability and foamability, and also demonstrated superior elasticity. Therefore, this foam formulation was selected to conduct foam flooding tests using a consolidated sand pack sample representing contaminated groundwater-bearing formations. Decane was employed as the non-aqueous phase liquid (NAPL) contaminant for the flooding tests. The foam injected by the pre-generation technique was generated using a sand-pack generator and injected into the consolidated sand-pack. Repeated experiments involving both water and foam injections revealed that foam injection resulted in approximately 68% contaminant recovery with only one pore volume of draining agent injection, whereas an equivalent volume of water injections yielded only around 19% decane recovery. Therefore, this foam, formulated by biosurfactant and bionanocrystals, can be a biodegradable and eco-friendly alternative for foams used for subsurface remediation. In the future, this

Orujov et al. Page 16 of 20

study could be expanded to include more biosurfactants and explore a wider range of foam properties in a bio-based system.

## STATEMENTS AND DECLARATIONS

# Acknowledgements

The authors would like to express their sincere gratitude to Director Trina Pfeiffer of the School of Energy Resources Center for Carbon Capture and Conversion for providing access to the rheology equipment.

#### **Author Contributions**

A.O.: Methodology, Software, Validation, Formal Analysis, Investigation, Data Curation, Visualization, Writing – Original Draft; B.A.: Methodology, Validation, Investigation, Writing – Original Draft; K.W.: Conceptualization, Writing – Review & Editing; S.A.A.: Conceptualization, Methodology, Resources, Writing – Review & Editing, Supervision, Project Administration, Funding Acquisition.

# **Conflicts of Interest**

The authors declare no competing interest.

# **Data, Code & Protocol Availability**

Data will be made available upon request.

# **Funding Received**

The corresponding author gratefully acknowledges the support of the University of Wyoming College of Engineering and Physical Sciences through its Engineering Initiative. KW and SAA thank the Faculty Grant-In-Aid from the University of Wyoming Office of Research and Economic Development, which supported the purchase of the rhamnolipids used in this study.

# **ORCID IDs**

Alirza Orujov

Behbood Abedi

Karen Wawrousek
Saman Aryana

| https://orcid.org/0009-0009-4082-3094 |
| https://orcid.org/0000-0002-4280-5259 |
| https://orcid.org/0000-0002-0764-703X |
| https://orcid.org/0000-0001-9509-7420 |

#### June 4, 2025:

The original online PDF has been replaced with an updated version featuring enlarged figures for improved clarity and easier reading.

# **REFERENCES**

- 1. Abedi, B., Orujov, A., Dabbaghi, E., Ng, K., Ackerman, J., & Aryana, S. A. (2024). Containment strategy for subsurface H2 storage based on time-dependent soft solids. *International Journal of Hydrogen Energy*, 82, 1001-1014. https://doi.org/10.1016/j.ijhydene.2024.07.336
- 2. Adegbola, A. A., Olajide, G., Mudashiru, L. O., & Adeaga, O. A. (2018). Numerical Investigation of Enhanced Oil Recovery with Steam Injection. *International Journal of Management, IT and Engineering*, 8(5), 1-24.
- 3. Aggelopoulos, C. A., Tsakiroglou, C. D., Ognier, S., & Cavadias, S. (2015). Non-aqueous phase liquid-contaminated soil remediation by ex situ dielectric barrier discharge plasma. *International Journal of Environmental Science and Technology*, 12, 1011-1020. https://doi.org/10.1007/s13762-013-0489-4
- 4. AlYousef, Z., Almobarky, M., & Schechter, D. (2017). Enhancing the stability of foam by the use of nanoparticles. *Energy & Fuels*, 31(10), 10620-10627. https://doi.org/10.1021/acs.energyfuels.7b01697

Orujov et al. Page 17 of 20

5. Apaydin, O. G., & Kovscek, A. R. (2001). Surfactant concentration and end effects on foam flow in porous media. *Transport in Porous Media*, 43(3), 511–536. https://doi.org/10.1023/A:1010740811277

- 6. Aranda, R., Davarzani, H., Colombano, S., Laurent, F., & Bertin, H. (2020). Experimental study of foam flow in highly permeable porous media for soil remediation. *Transport in Porous Media*, 134(1), 231-247. https://doi.org/10.1007/s11242-020-01443-8
- Arkhipov, V. P., Arkhipov, R., & Filippov, A. (2023). Rhamnolipid biosurfactant: Use for the removal of phenol from aqueous solutions by micellar solubilization. ACS Omega, 8(33), 30646–30654. https://doi.org/10.1021/acsomega.3c04367
- 8. Atteia, O., Jousse, F., Cohen, G., & Höhener, P. (2017). Comparison of residual NAPL source removal techniques in 3D metric scale experiments. *Journal of Contaminant Hydrology*, 202, 23-32. https://doi.org/10.1016/j.jconhyd.2017.04.006
- 9. Bazsefidpar, S., Mokhtarani, B., Panahi, R., & Hajfarajollah, H. (2019). Overproduction of rhamnolipid by fedbatch cultivation of Pseudomonas aeruginosa in a lab-scale fermenter under tight DO control. *Biodegradation*, 30(1), 59–69. https://doi.org/10.1007/s10532-018-09866-3
- Brinchi, L., Cotana, F., Fortunati, E., & Kenny, J. M. (2013). Production of nanocrystalline cellulose from lignocellulosic biomass: Technology and applications. *Carbohydrate Polymers*, 94(1), 154–169. https://doi.org/10.1016/j.carbpol.2013.01.033
- 11. Cavelan, A., Faure, P., Lorgeoux, C., Colombano, S., Deparis, J., et al. (2024). An experimental multi-method approach to better characterize the LNAPL fate in soil under fluctuating groundwater levels. *Journal of Contaminant Hydrology*, 104319. https://doi.org/10.1016/j.jconhyd.2024.104319
- 12. Chen, I.-C., & Lee, M.-T. (2022). Rhamnolipid biosurfactants for oil recovery: Salt effects on the structural properties investigated by mesoscale simulations. *ACS Omega*, 7(7), 6223–6237. https://doi.org/10.1021/acsomega.1c06741
- 13. Davoodi, S., Al-Shargabi, M., Wood, D. A., Mehrad, M., & Rukavishnikov, V. S. (2024). Carbon dioxide sequestration through enhanced oil recovery: A review of storage mechanisms and technological applications. *Fuel*, 366, 131313. https://doi.org/10.1016/j.fuel.2024.131313
- 14. Desai, J. D., & Banat, I. M. (1997). Microbial production of surfactants and their commercial potential. *Microbiology and Molecular Biology Reviews*, 61(1), 47–64. https://doi.org/10.1128/mmbr.61.1.47-64.1997
- 15. Domingues, R. M. A., Gomes, M. E., & Reis, R. L. (2014). The potential of cellulose nanocrystals in tissue engineering strategies. *Biomacromolecules*, 15(7), 2327–2346. https://doi.org/10.1021/bm500524s
- 16. Du, D., Zhang, X., Yu, K., Song, X., Shen, Y., et al. (2020). Parameter screening study for optimizing the static properties of nanoparticle-stabilized CO<sub>2</sub> foam based on orthogonal experimental design. *ACS Omega*, 5(8), 4014-4023. https://doi.org/10.1021/acsomega.9b03543
- 17. Emami, H., Ayatizadeh Tanha, A., Khaksar Manshad, A., & Mohammadi, A. H. (2022). Experimental investigation of foam flooding using anionic and nonionic surfactants: A screening scenario to assess the effects of salinity and pH on foam stability and foam height. *ACS Omega*, 7(17), 14832–14847. https://doi.org/10.1021/acsomega.2c00314
- 18. Emrani, A. S., & Nasr-El-Din, H. A. (2015). Stabilizing CO2-foam using nanoparticles. Paper presented at the SPE European Formation Damage Conference and Exhibition. OnePetro. https://doi.org/10.2118/174254-MS
- 19. Farajzadeh, R., Krastev, R., & Zitha, P. L. J. (2008). Foam films stabilized with alpha olefin sulfonate (AOS). *Colloids and Surfaces Physicochemical and Engineering Aspects*, 324(1), 35–40. https://doi.org/10.1016/j.colsurfa.2008.03.024
- 20. Fei-Baffoe, B., Badu, E., Miezah, K., Sackey, L. N. A., Sulemana, A., & Amuah, E. E. Y. (2024). Contamination of groundwater by petroleum hydrocarbons: Impact of fuel stations in residential areas. *Heliyon*, 10(4). https://doi.org/10.1016/j.heliyon.2024.e25924
- 21. Forey, N., Atteia, O., Omari, A., & Bertin, H. (2020). Saponin foam for soil remediation: On the use of polymer or solid particles to enhance foam resistance against oil. *Journal of Contaminant Hydrology*, 228, 103560. https://doi.org/10.1016/j.jconhyd.2019.103560
- 22. George, J., & Sabapathi, S. N. (2015). Cellulose nanocrystals: Synthesis, functional properties, and applications. *Nanotechnology Science and Applications*, 8, 45–54. https://doi.org/10.2147/NSA.S64386
- 23. Ghezzi, M., Pescina, S., Padula, C., Santi, P., Del Favero, E., Cantù, L., & Nicoli, S. (2021). Polymeric micelles in drug delivery: An insight of the techniques for their characterization and assessment in biorelevant conditions. *Journal of Controlled Release*, 332, 312-336. https://doi.org/10.1016/j.jconrel.2021.02.031
- 24. Gong, Z., Yang, G., Che, C., Liu, J., Si, M., & He, Q. (2021). Foaming of rhamnolipids fermentation: impact factors and fermentation strategies. *Microbial Cell Factories*, 20, 1-12. https://doi.org/10.1186/s12934-021-01516-3
- 25. Grassian, V. H., O'Shaughnessy, P. T., Adamcakova-Dodd, A., Pettibone, J. M., & Thorne, P. S. (2007). Inhalation exposure study of titanium dioxide nanoparticles with a primary particle size of 2 to 5 nm. *Environmental Health Perspectives*, 115(3), 397–402. https://doi.org/10.1289/ehp.9469

Orujov et al. Page 18 of 20

26. Guimbaud, C., Colombano, S., Noel, C., Verardo, E., Grossel, A., et al. (2023). Quantification of biodegradation rate of hydrocarbons in a contaminated aquifer by CO2 δ13C monitoring at ground surface. *Journal of Contaminant Hydrology*, 256, 104168. https://doi.org/10.1016/j.jconhyd.2023.104168

- 27. Guo, F., & Aryana, S. (2016). An experimental investigation of nanoparticle-stabilized CO2 foam used in enhanced oil recovery. *Fuel*, 186, 430–442. https://doi.org/10.1016/j.fuel.2016.08.058
- 28. Guo, F., He, J., Johnson, P. A., & Aryana, S. A. (2017). Stabilization of CO2 foam using by-product fly ash and recyclable iron oxide nanoparticles to improve carbon utilization in EOR processes. *Sustainable Energy & Fuels*, 1(4), 814–822. https://doi.org/10.1039/C7SE00098G
- 29. Harwell, J. H., Sabatini, D. A., & Knox, R. C. (1999). Surfactants for ground water remediation. *Colloids and Surfaces A: Physicochemical and Engineering Aspects*, 151(1-2), 255-268. https://doi.org/10.1016/S0927-7757(98)00785-7
- 30. Hassanshahian, M. (2014). Isolation and characterization of biosurfactant producing bacteria from Persian Gulf (Bushehr provenance). *Marine Pollution Bulletin*, 86(1), 361–366. https://doi.org/10.1016/j.marpolbul.2014.06.043
- 31. Hollenbach, R., Oeppling, S., Delavault, A., Völp, A. R., Willenbacher, N., et al. (2021). Comparative study on interfacial and foaming properties of glycolipids in relation to the gas applied for foam generation. *RSC advances*, 11(54), 34235-34244. https://doi.org/10.1039/D1RA06190A
- 32. Imron, M. F., Kurniawan, S. B., Ismail, N. 'Izzati., & Abdullah, S. R. S. (2020). Future challenges in diesel biodegradation by bacteria isolates: A review. *Journal of Cleaner Production*, 251, 119716. https://doi.org/10.1016/j.jclepro.2019.119716
- 33. Invally, K., Sancheti, A., & Ju, L.-K. (2019). A new approach for downstream purification of rhamnolipid biosurfactants. *Food and Bioproducts Processing*, 114, 122–131. https://doi.org/10.1016/j.fbp.2018.12.003
- 34. Ishigami, Y., Gama, Y., Ishii, F., & Choi, Y. K. (1993). Colloid chemical effect of polar head moieties of a rhamnolipid-type biosurfactant. Langmuir, 9(7), 1634-1636. https://doi.org/10.1021/la00031a006
- 35. Jangir, K., Kumar, U., Suniya, N. K., Singh, N., & Parihar, K. (2022). Enhancing the Aqueous foam Stability Using Nanoparticles: A Review. *World*, 10(2), 84-90. https://doi.org/10.12691/wjce-10-2-5
- 36. Janssen, M., Mutawa, A., Pilus, R., & Zitha, P. (2019). Evaluation of foam-assisted surfactant flooding at reservoir conditions. Paper presented at the SPE Europec featured at 81st EAGE Conference and Exhibition. OnePetro. https://doi.org/10.2118/195481-MS
- 37. Karlsson, H. L., Cronholm, P., Gustafsson, J., & Möller, L. (2008). Copper oxide nanoparticles are highly toxic: A comparison between metal oxide nanoparticles and carbon nanotubes. *Chemical Research in Toxicology*, 21(9), 1726–1732. https://doi.org/10.1021/tx800064j
- 38. Khajehpour, M., Reza Etminan, S., Goldman, J., Wassmuth, F., & Bryant, S. (2018). Nanoparticles as foam stabilizer for steam-foam process. *SPE Journal*, 23(06), 2232-2242. https://doi.org/10.2118/179826-PA
- 39. Kim, I., Worthen, A. J., Johnston, K. P., DiCarlo, D. A., & Huh, C. (2016). Size-dependent properties of silica nanoparticles for Pickering stabilization of emulsions and foams. *Journal of Nanoparticle Research*, 18, 1-12. https://doi.org/10.1007/s11051-016-3395-0
- 40. Kwon, H., Mohamed, M. M., Annable, M. D., & Kim, H. (2020). Remediation of NAPL-contaminated porous media using micro-nano ozone bubbles: Bench-scale experiments. *Journal of Contaminant Hydrology*, 228, 103563. https://doi.org/10.1016/j.jconhyd.2019.103563
- 41. Li, R. F., Yan, W., Liu, S., Hirasaki, G. J., & Miller, C. A. (2010). Foam mobility control for surfactant enhanced oil recovery. *SPE Journal*, 15(04), 928–942. https://doi.org/10.2118/113910-PA
- 42. Longpré-Girard, M., Martel, R., Robert, T., Lefebvre, R., Lauzon, J. M., & Thomson, N. (2020). Surfactant foam selection for enhanced light non-aqueous phase liquids (LNAPL) recovery in contaminated aquifers. *Transport in Porous Media*, 131, 65-84. https://doi.org/10.1007/s11242-019-01292-0
- 43. Lunkenheimer, K., & Malysa, K. (2003). Simple and generally applicable method of determination and evaluation of foam properties. *Journal of Surfactants and Detergents*, 6(1), 69–74. https://doi.org/10.1007/s11743-003-0251-8
- 44. Majeed, T., Sølling, T. I., & Kamal, M. S. (2020). Foam stability: The interplay between salt-, surfactant- and critical micelle concentration. *Journal of Petroleum Science and Engineering*, 187, 106871. https://doi.org/10.1016/j.petrol.2019.106871
- 45. Masarudin, M. J., Cutts, S. M., Evison, B. J., Phillips, D. R., & Pigram, P. J. (2015). Factors determining the stability, size distribution, and cellular accumulation of small, monodisperse chitosan nanoparticles as candidate vectors for anticancer drug delivery: application to the passive encapsulation of (14C)-doxorubicin. *Nanotechnology, Science and Applications*, 67-80. https://doi.org/10.2147/NSA.S91785
- 46. Meyers, R. A. (2012). Encyclopedia of sustainability science and technology (Vol. 6). New York: Springer. https://doi.org/10.1007/978-1-4419-0851-3

Orujov et al. Page 19 of 20

47. Nadim, F., Hoag, G. E., Liu, S., Carley, R. J., & Zack, P. (2000). Detection and remediation of soil and aquifer systems contaminated with petroleum products: an overview. *Journal of Petroleum Science and Engineering*, 26(1-4), 169-178. https://doi.org/10.1016/S0920-4105(00)00031-0

- 48. Nurfarahin, A. H., Mohamed, M. S., & Phang, L. Y. (2018). Culture medium development for microbial-derived surfactants production—An overview. Molecules, 23(5). https://doi.org/10.3390/molecules23051049
- 49. Orujov, A., Coddington, K., & Aryana, S. A. (2023). A review of CCUS in the context of foams, regulatory frameworks and monitoring. *Energies*, 16(7), 3284. https://doi.org/10.3390/en16073284
- 50. Özdemir, G., Peker, S., & Helvaci, S. S. (2004). Effect of pH on the surface and interfacial behavior of rhamnolipids R1 and R2. *Colloids and Surfaces A: Physicochemical and Engineering Aspects*, 234(1-3), 135-143. https://doi.org/10.1016/j.colsurfa.2003.10.024
- 51. Paneiro, G., & Orujov, A. (2023, May). Absolute Permeability of Codaçal Porous Limestone Under Different Pressure and Temperature Conditions. In: Advances in Geoengineering, Geotechnologies, and Geoenvironment for Earth Systems and Sustainable Georesources Management: *Proceedings of the 1st Conference on Georesources, Geomaterials, Geotechnologies and Geoenvironment (4GEO)*, Porto, 2019 (pp. 69-74). Cham: Springer International Publishing. https://doi.org/10.1007/978-3-031-25986-9\_11
- 52. Rahman, A., Torabi, F., & Shirif, E. (2023). Surfactant and nanoparticle synergy: Towards improved foam stability. *Petroleum*, 9(2), 255-264. https://doi.org/10.1016/j.petlm.2023.02.002
- 53. Ray, P. C., Yu, H., & Fu, P. P. (2009). Toxicity and environmental risks of nanomaterials: Challenges and future needs. *Journal of Environmental Science and Health Part C*, 27(1), 1–35. https://doi.org/10.1080/10590500802708267
- 54. Rezk, M. Y., & Allam, N. K. (2019). Impact of nanotechnology on enhanced oil recovery: A mini-review. *Industrial & Engineering Chemistry Research*, 58(36), 16287–16295. https://doi.org/10.1021/acs.iecr.9b03693
- 55. Roadcap, G. S., Kelly, W. R., & Bethke, C. M. (2005). Geochemistry of extremely alkaline (pH> 12) ground water in slag-fill aquifers. *Groundwater*, 43(6), 806-816. https://doi.org/10.1111/j.1745-6584.2005.00060.x
- Rodrigues, L. R. (2015). Microbial surfactants: Fundamentals and applicability in the formulation of nano-sized drug delivery vectors. *Journal of Colloid and Interface Science*, 449, 304–316. https://doi.org/10.1016/j.jcis.2015.01.022
- 57. Sánchez, M., Aranda, F. J., Espuny, M. J., Marqués, A., Teruel, J. A., Manresa, Á., & Ortiz, A. (2007). Aggregation behaviour of a dirhamnolipid biosurfactant secreted by Pseudomonas aeruginosa in aqueous media. *Journal of Colloid and Interface science*, 307(1), 246-253. https://doi.org/10.1016/j.jcis.2006.11.041
- 58. Shankaran, D. R. (2018). Chapter 14 Cellulose nanocrystals for health care applications. In: S. Mohan Bhagyaraj, O. S. Oluwafemi, N. Kalarikkal, & S. Thomas (Eds.), Applications of Nanomaterials (pp. 415–459). *Micro and Nano Technologies.* Woodhead Publishing. https://doi.org/10.1016/B978-0-08-101971-9.00015-6
- 59. Shojaei, M. J., Méheust, Y., Osman, A., Grassia, P., & Shokri, N. (2021). Combined effects of nanoparticles and surfactants upon foam stability. *Chemical engineering science*, 238, 116601. https://doi.org/10.1016/j.ces.2021.116601
- 60. Slessarev, E. W., Lin, Y., Bingham, N. L., Johnson, J. E., Dai, Y., Schimel, J. P., & Chadwick, O. A. (2016). Water balance creates a threshold in soil pH at the global scale. *Nature*, 540(7634), 567-569. https://doi.org/10.1038/nature20139
- 61. Soberón-Chávez, G., González-Valdez, A., Soto-Aceves, M. P., & Cocotl-Yañez, M. (2021). Rhamnolipids produced by Pseudomonas: From molecular genetics to the market. *Microbial Biotechnology*, 14(1), 136–146. https://doi.org/10.1111/1751-7915.13700
- 62. Topel, Ö., Çakır, B. A., Budama, L., & Hoda, N. (2013). Determination of critical micelle concentration of polybutadiene-block-poly(ethyleneoxide) diblock copolymer by fluorescence spectroscopy and dynamic light scattering. *Journal of Molecular Liquids*, 177, 40–43. https://doi.org/10.1016/j.molliq.2012.10.013
- 63. Vecino, X., Cruz, J. M., Moldes, A. B., & Rodrigues, L. R. (2017). Biosurfactants in cosmetic formulations: Trends and challenges. *Critical Reviews in Biotechnology*, 37(7), 911–923. https://doi.org/10.1080/07388551.2016.1269053
- 64. Vidonish, J. E., Zygourakis, K., Masiello, C. A., Sabadell, G., & Alvarez, P. J. J. (2016). Thermal treatment of hydrocarbon-impacted soils: A review of technology innovation for sustainable remediation. *Engineering*, 2(4), 426–437. https://doi.org/10.1016/J.ENG.2016.04.005
- 65. Wang, R., Arshadi, M., Zankoor, A., & Piri, M. (2022). Pore Space Deformation and its Implications for Two-Phase Flow Through Porous Media: A Micro-Scale Experimental Investigation. *Water Resources Research*, 58(10), e2022WR032157. https://doi.org/10.1029/2022WR032157
- Wang, S., & Mulligan, C. N. (2004). Rhamnolipid foam enhanced remediation of cadmium and nickel contaminated soil. *Water, Air, and Soil Pollution*, 157, 315-330. https://doi.org/10.1023/B:WATE.0000038904.91977.f0

Orujov et al. Page 20 of 20

67. Wang, Z., Sun, J., Wang, Y., Guo, H., & Aryana, S. A. (2021). Optimum concentration of fly ash nanoparticles to stabilize CO2 foams for aquifer and soil remediation. *Journal of Contaminant Hydrology*, 242, 103853. https://doi.org/10.1016/j.jconhyd.2021.103853

- 68. Whang, L.-M., Liu, P.-W. G., Ma, C.-C., & Cheng, S.-S. (2009). Application of rhamnolipid and surfactin for enhanced diesel biodegradation—Effects of pH and ammonium addition. *Journal of Hazardous Materials*, 164(2), 1045–1050. https://doi.org/10.1016/j.jhazmat.2008.09.006
- 69. Wu, L. M., Lai, L., Lu, Q., Mei, P., Wang, Y. Q., Cheng, L., & Liu, Y. (2019). Comparative studies on the surface/interface properties and aggregation behavior of mono-rhamnolipid and di-rhamnolipid. *Colloids and Surfaces B: Biointerfaces*, 181, 593-601. https://doi.org/10.1016/j.colsurfb.2019.06.012
- 70. Xia, T., Ma, M., Huisman, J. A., Zheng, C., Gao, C., & Mao, D. (2023). Monitoring of in-situ chemical oxidation for remediation of diesel-contaminated soil with electrical resistivity tomography. *Journal of Contaminant Hydrology*, 256, 104170. https://doi.org/10.1016/j.jconhyd.2023.104170
- 71. Xu, Q., Nakajima, M., Ichikawa, S., Nakamura, N., Roy, P., Okadome, H., & Shiina, T. (2009). Effects of surfactant and electrolyte concentrations on bubble formation and stabilization. *Journal of Colloid and Interface science*, 332(1), 208-214. https://doi.org/10.1016/j.jcis.2008.12.044
- 72. Xu, Z., Li, B., Zhao, H., He, L., Liu, Z., Chen, D., ... & Li, Z. (2020). Investigation of the effect of nanoparticle-stabilized foam on EOR: nitrogen foam and methane foam. *ACS Omega*, 5(30), 19092-19103. https://doi.org/10.1021/acsomega.0c02434
- 73. Xue, S. W., Huang, C., Tian, Y. X., Li, Y. B., Li, J., & Ma, Y. L. (2020). Synergistic effect of rhamnolipids and inoculation on the bioremediation of petroleum-contaminated soils by bacterial consortia. *Current Microbiology*, 77, 997-1005. https://doi.org/10.1007/s00284-020-01899-3
- 74. Yang, W., Wang, T., Fan, Z., Miao, Q., Deng, Z., & Zhu, Y. (2017). Foams stabilized by in situ-modified nanoparticles and anionic surfactants for enhanced oil recovery. *Energy & Fuels*, 31(5), 4721-4730. https://doi.org/10.1021/acs.energyfuels.6b03217
- 75. Yekeen, N., Manan, M. A., Idris, A. K., & Samin, A. M. (2017). Influence of surfactant and electrolyte concentrations on surfactant Adsorption and foaming characteristics. *Journal of Petroleum Science and Engineering*, 149, 612-622. https://doi.org/10.1016/j.petrol.2016.11.018
- 76. Zhang, Y., Liu, Q., Ye, H., Yang, L., Luo, D., & Peng, B. (2021). Nanoparticles as foam stabilizer: Mechanism, control parameters and application in foam flooding for enhanced oil recovery. *Journal of Petroleum Science and Engineering*, 202, 108561. https://doi.org/10.1016/j.petrol.2021.108561
- 77. Zhu, Y., Wang, X., Zhang, Y., Chio, C., Qin, W., & Li, H. (2023). Surfactant-containing foam effectively enhanced the removal of polycyclic aromatic hydrocarbons from heavily contaminated soil. *Bulletin of Environmental Contamination and Toxicology*, 110(2), 50. https://doi.org/10.1007/s00128-022-03672-7